ISSN 0021-3640, JETP Letters, 2022, Vol. 115, No. 9, pp. 531–538. © Pleiades Publishing, Inc., 2022.
Russian Text © The Author(s), 2022, published in Pis'ma v Zhurnal Eksperimental'noi i Teoreticheskoi Fiziki, 2022, Vol. 115, No. 9, pp. 585–592.

CONDENSED MATTER

Effect of the Oxygen Content on the Metal–Insulator Transition and on the Spin State of Co^{3+} Ions in the Layered $NdBaCo_2O_{5+\delta}$ Cobaltite ($0.37 \le \delta \le 0.65$)

N. I. Solin[a], * and S. V. Naumov[a]

[a] *Mikheev Institute of Metal Physics, Ural Branch, Russian Academy of Sciences, Yekaterinburg, 620108 Russia*
**e-mail: solin@imp.uran.ru*

Received January 17, 2022; revised March 25, 2022; accepted March 26, 2022

The effect of the oxygen content δ in layered $NdBaCo_2O_{5+\delta}$ cobaltite, where $0.37 \le \delta \le 0.65$, on the metal–insulator transition, as well as on the magnetic and spin states of Co^{3+}, is studied for the first time. An increase in δ reduces the metal–insulator transition temperature T_{MI}, the antiferromagnetic ordering temperature T_N, and the Curie temperature T_C by about 100–150 K. For all values of δ, the metal–insulator transition occurs when the spin state of Co^{3+} ions changes from the HS/LS state in the metallic phase to the IS/LS state in the semiconducting phase, whereas with an increase in δ, the spin state of Co^{3+} ions changes from the IS/LS to HS/LS state. At $\delta \sim 0.65$, a heavily doped semiconductor–bad metal transition occurs without any change in the spin state of Co^{3+} ions. The ferromagnetic behavior of $NdBaCo_2O_{5+\delta}$ in the antiferromagnetic phase below T_N is interpreted in terms of the metamagnetic model as the effect of the size of the rare earth Nd^{3+} ion on the antiferromagnetic state in layered cobaltites.

DOI: 10.1134/S0021364022100472

INTRODUCTION

Broad interest in ordered layered $RBaCo_2O_{5+\delta}$ cobalt oxides, where R stands for a R^{3+} rare earth ion and δ is the oxygen content, is due to their unusual magnetic and transport properties [1, 2]. They have the layered perovskite-type crystal structure, consisting of layers located along the *c* axis, in which RO_δ and BaO layers alternate with CoO_2 layers. $RBaCo2O_{5+\delta}$ compounds with $\delta \approx 0.5$, where R = Eu, Gd, Tb, etc., from the middle of the rare earth row, are studied in the most detail [1–7]. $RCo_2O_{5.5}$ contains only Co^{3+} ions, which are located in the crystal lattice within an equal number of CoO_6 octahedra and square CoO_5 pyramids [1]. They exhibit a number of successive metal–insulator (MI), paramagnetic (PM), ferromagnetic (FM), and antiferromagnetic (AFM) phase transitions [1–7].

The main problem concerns the nature and driving forces of the metal–insulator transition in these materials. In contrast to manganites, the MI transition in cobaltites is not related to magnetic ordering. The properties of $RBaCo_2O_{5+\delta}$ compounds, as well as of $LaCoO_3$, are unusual mainly because cobalt ions can be in three different states: low-spin (LS), intermediate-spin (IS), and high-spin (HS) states. The energy differences between the spin states are mostly small [8] and can be easily overcome with a change in the temperature, forming unusual sequences of structural and other phase transitions, including the MI transition. The structural and magnetic data [4] indicate that, in $GdBaCo_2O_{5.5}$, the transition from the insulating to the metallic phase is related to the excitation of electrons from the LS state to the HS state corresponding to the e_g band formed by Co^{3+} ions in octahedra without any changes in the IS state of Co^{3+} in pyramids. Although this model contradicts the structural data, it is widely accepted. Many researchers adhere to this model of the metal–insulator transition in other $RBaCo_2O_{5.50}$ cobaltites as well. Refinement of the paramagnetic contribution of R^{3+} ions shows [9] that the transition can occur when the spin states of Co^{3+} ions in octahedra and pyramids change, in agreement with the structural data [4].

The size of the rare earth ion affects the crystal field at the Co ions and, therefore, it can change their spin state and the magnetic state of $RBaCo_2O_{5.5}$ [10]. The largest rare earth ions are Pr^{3+} and Nd^{3+} [11]. The neutron and synchrotron X-ray powder diffraction data [12] and muon spectroscopy data [13] show that, although the phase transition temperatures in $NdBaCo_2O_{5.5}$ are similar to those of known cobaltites, their microscopic magnetic nature is quite different. In particular, the FM state is retained in $NdBaCo_2O_{5+\delta}$

with $\delta \approx 0.5$ [14] and $PrBaCo_2O_{5.50}$ [15] below $T_N \sim 230-250$ K, while other cobaltites remain in the AFM state [1–7]. The metamagnetic state and ferromagnetic behavior of $NdBaCo_2O_{5+\delta}$ with $\delta \approx 0.5$ at low temperatures is explained in [14] within the Landau model of metamagnetism [16] by the large size of rare earth ions and by the spin-state ordering (SSO) of Co^{3+} ions below $T \sim T_{SSO}$ [12, 17–19].

The oxygen content δ in $RBaCo_2O_{5+\delta}$, which can be varied in a wide range $0 \le \delta \le 1$, plays an important role [1]. It controls not only the average valency of Co ions (which can vary from 3.5+ for $\delta = 1$ to 2.5+ for $\delta = 0$) but also their oxygen (pyramidal or octahedral) environment and therefore has a strong effect on the spin state of Co ions. As a result, the magnetic and transport characteristics of these compounds are largely determined by the oxygen content [1–7].

Much less is known about the properties of $RBaCo_2O_{5+\delta}$ compounds with higher oxygen content $\delta > 0.5$. The properties of electron- ($\delta < 0.5$) and hole-doped ($\delta > 0.5$) $GdBaCo_2O_{5+\delta}$ single crystals are asymmetric. With an increase in the density of charge carriers in electron-doped compounds, the electrical resistivity increases and the magnetization decreases, and in the hole-doped ones, the electrical resistance decreases and the magnetization increases [3]. There are several studies of $RBaCo_2O_{5+\delta}$ compounds with a fixed composition, where R = Nd, Pr and $\delta \sim 0.7$ [20–22]. Near the metal–insulator transition, the resistivity of $NdBaCo_2O_{5+\delta}$ at $\delta \approx 0.7$ has an activation character [20]. The magnetic properties and paramagnet–ferromagnet phase diagram of $PrBaCo_2O_{5+\delta}$, where $0.35 \le \delta \le 0.8$, are unusual and differ from the properties of known layered cobaltites [15]. The metal–insulator transition in $PrBaCo_2O_{5+\delta}$, where $0.5 \le \delta \le 0.7$, is explained by a change in the spin states of Co^{3+} ions [19]. It is of interest to compare the properties of $PrBaCo_2O_{5+\delta}$ [15, 19] and of the related $NdBaCo_2O_{5+\delta}$ compound at different oxygen contents.

In this work, we present the results of our studies on the effect of the oxygen content on the PM–FM (T_C), FM–AFM (T_N), and metal–insulator transitions and on their relation to the change in the Co^{3+} spin states in $NdBaCo_2O_{5+\delta}$ polycrystals, where $0.37 \le \delta \le 0.65$. The paramagnetic contribution of the Nd^{3+} rare earth ions is taken into account, in contrast to other well-known works [15, 19, 21, 22]. It is found that the spin state of Co^{3+} ions in the metallic phase of $NdBaCo_2O_{5+\delta}$ cobaltite is independent of δ, whereas the effective magnetic moment μ_{eff}/Co below the MI transition temperature increases with δ, approaching the value corresponding to the spin state of the metallic phase in $NdBaCo_2O_{5+\delta}$.

RESULTS

$NdBaCo_2O_{5+\delta}$ polycrystals were synthesized by the solid-state reaction technique using Nd_2O_3, $BaCO_3$, and Co_3O_4 as initial components. The preparation process includes stepwise annealing in air at $T = 900-1125$°C and slow cooling down to room temperature [1]. The absolute oxygen content was determined by the method of sample reduction in hydrogen. The initial samples had the oxygen content $\delta = 0.65 \pm 0.02$. The required oxygen content δ was achieved by additional annealing of the original sample at $T = 350-800$°C followed by quenching and was determined from the change in the sample weight [3], under the assumption that $\delta = 0.65$. The weight of the samples was chosen such that the accuracy of determining δ was no worse than 0.01. According to the X-ray powder diffraction data, all samples were single-phase. At room temperature, the samples with $\delta = 0.48-0.65$ have an orthorhombic structure and are described by the space group *Pmmm* (no. 47) with the $a_p \times 2a_p \times 2a_p$ unit cell, where a_p is the pseudocubic perovskite lattice constant. The sample with $\delta = 0.37$ also has the orthorhombic structure (no. 47) with the $a_p \times a_p \times 2a_p$ unit cell. The unit cell volume decreases with an increase in δ. The structural parameters of the samples agree with the published data [23]. The resistivity was measured by the four-probe method. The magnetic measurements were performed using the MPMS-5XL (Quantum Design) facility at the Shared Research Center, Mikheev Institute of Metal Physics, Ural Branch, Russian Academy of Sciences.

In Fig. 1, we show the temperature dependence of the magnetization of six $NdBaCo_2O_{5+\delta}$ samples with δ ranging from 0.37 to 0.65. At $\delta \ne 0.5$, in addition to Co^{3+} ions, Co^{2+} or Co^{4+} ions with the content $|\delta - 0.5|$ appear. The samples were cooled at zero magnetic field from 300 K to 10 K and measured in the magnetic field $H = 1$ kOe at temperatures up to 400 K. The form of the magnetization curves $M(T)$ turns out to be nearly the same for all known layered $RBaCo_2O_{5.5}$ cobaltites. The magnetization increases sharply below $T_C \sim 280$ K. Within a narrow temperature range, the sample appears to be in the FM state, where $M(T)$ has the maximum at $T_{max} = T_N \sim 250$ K, below which it decreases gradually, suggesting the transition of the sample to the AFM state [1–7].

The presented temperature dependences of the magnetization $M(T)$ of $NdBaCo_2O_{5+\delta}$ differ from those characteristic of known layered $RBaCo_2O_{5.5}$ cobaltite, in which the transition temperatures to FM (T_C) and AFM (T_N) are nearly independent of the choice of R [1–7]. As the oxygen content increases, the magnetization peak $M_{max}(\delta)$ at T_N changes nonmonotonically, exhibiting a minimum at $\delta = 0.60$; then it increases, and the T_N values become strongly lower (Fig. 1). The Curie temperature $T_C(\delta)$, determined from the maximum value of dM/dT (see inset

of Fig. 1), decreases with increasing oxygen content from 260 to 120 K and changes slightly up to $\delta = 0.53$, and $T_C(\delta)$ exhibits the maximum change at $\delta > 0.53$–0.60. The spontaneous magnetization M_s determined from $M(H)$ up to 50 kOe at $T =$ const appears about 15–20 K higher than the value T_C determined from the maximum of dM/dT; i.e., the magnetic order apparently arises at $T_C(\delta) \approx 280$–140 K. The formation of M_s at $T \sim 140$ K and $\delta = 0.65$ agrees with the data reported in [20]. The transition temperature to the AFM state, determined from the temperature of the magnetization peak $T_{max}(\delta) \approx T_N$, is approximately 20 K lower than $T_C(\delta)$, and the $T_C(\delta)$ dependence has a similar form (see the inset of Fig. 1).

The main difference between $NdBaCo_2O_{5+\delta}$ and known cobaltites, except for $PrBaCo_2O_{5+\delta}$ [15] and $LaBaCo_2O_{5.50}$ [24], is that the magnetization below $T_N(\delta)$ exhibits the ferromagnetic behavior and remains finite at nonzero magnetic field. The data on $M(T, H = 1$ kOe) below 175 K for $\delta = 0.37$–0.53 are not shown in Fig. 1, but the magnetization also remains finite, as for $\delta = 0.60$–0.65. In $PrBaCo_2O_{5+\delta}$ ($0.37 \le \delta \le 0.80$), the FM interactions are also present at all temperatures below T_C and even in the AFM phase [15].

The ferromagnetic behavior of $NdBaCo_2O_{5.48}$ below T_N was explained by the metamagnetic state of this compound [14]. Below $T \sim 20$ K, $NdBaCo_2O_{5.48}$ at zero magnetic field is in the AFM state, and in a low magnetic field of 10–20 kOe, it transforms to the metamagnetic state, i.e., to the mixed FM + AFM state. Above $T \sim 20$ K, the sample involves a mixture of exchange-coupled ferromagnetic and antiferromagnetic phases. This situation is confirmed by the discovery of an exchange bias in $NdBaCo_2O_{5.48}$ [14].

Layered cobaltites are AFM materials with weakly coupled spin sublattices [3] and are metamagnets even at high temperatures [7]. In $RBaCo_2O_{5.50}$, where R = Gd, Tb, at $T \sim T_N \sim 250$ K, the applied magnetic field reduces the AFM/FM transition temperature by about 1 K at $H_{cr} \sim 10$ kOe, and at $T = 0$, the field $H_{cr} \sim 200$–300 kOe is required to generate this transition [3, 7, 14].

At $T_N \sim 275$ K and at zero magnetic field, Co^{3+} ions in a similar $NdBaCo_2O_{5.47}$ compound are ordered, forming a G-type AFM structure [12]. In the temperature range $T_N \sim 275$ K $> T > T_{SSO} \sim 230$ K, Co^{3+} ions are located in two positions with the pyramidal and octahedral oxygen environments. Below $T_{SSO} \sim 230$ K, the AFM spin-state ordered (SSO) phase arises in $NdBaCo_2O_{5.47}$, in which Co^{3+} ions are in four different states: in two different octahedra and pyramids. Following the Landau model of metamagnetism [16], it was assumed that the FM bond in Co layers in the layered compounds in the SSO state remains strong, whereas the AFM bond between Co layers separated

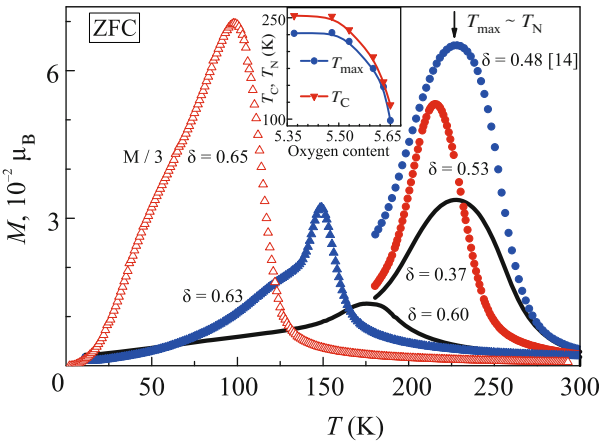

Fig. 1. (Color online) Temperature dependence of the magnetization of $NdBaCo_2O_{5+\delta}$, ($0.37 \le \delta \le 0.65$) at $H =$ 1 kOe. For clarity of images, the values of $M(T)$ for $\delta =$ 0.37–0.53 below 175 K are not shown. Their magnetization decreases monotonically with temperature. The inset demonstrates the dependence of the Curie temperature T_C and of the AFM ordering temperature T_N on the oxygen content. The PM contribution from Nd^{3+} ions is subtracted.

by NdO_δ layers is weakened because of a large size of Nd^{3+} ions. At not a high magnetic field, the transition between the AFM and FM states occurs.

We assume that such a model is also applicable at $\delta \approx 0.37$–0.65. Note that the effect of the oxygen content δ on T_C and T_N in $RBaCo_2O_{5+\delta}$ with R = Gd [3], Pr [15], and Nd (see the inset of Fig. 1) is nearly the same: the values of $T_C(\delta)$ and $T_N(\delta)$ vary only slightly at $\delta \approx 0.35$–0.5 and decrease strongly (by ~100 K) at $\delta = 0.5$–0.7. For the composition with $\delta = 0.7$, the FM order in $GdBaCo_2O_{5+\delta}$ also arises at temperatures $T < 150$ K, and an abrupt transition from the FM to AFM state occurs at $T < 100$ K [3], in contrast to $NdBaCo_2O_{5+\delta}$ and $PrBaCo_2O_{5+\delta}$ [15]. In $LaBaCo_2O_{5.50}$, where La is the largest nonmagnetic rare earth ion [11], the FM behavior below T_N is also explained by the effect of the size of the La^{3+} ion [24]. $RBaCo_2O_{5+\delta}$ compounds with $\delta = 1$ and R = Pr and La are ferromagnets with $T_C = 210$ and 179 K, respectively [25, 26]. The formation of the ferromagnetic state below T_N in $RBaCo_2O_{5+\delta}$ with R = La, Pr [24–26], and Nd having a large ionic radius and its absence in the $GdBaCo_2O_{5+\delta}$ compound [3] with a smaller ionic radius suggest that the ferromagnetic state of $NdBaCo_2O_{5+\delta}$ below T_N is determined by the large size of Nd^{3+} ions.

The exchange bias detected in $NdBaCo_2O_{5+\delta}$ at $\delta = 0.37$–0.53 and $T = 77$ K indicates the phase separation in this compound into exchange-coupled FM and AFM phases, which is characteristic of the metamagnetic state, and thus supports this assumption.

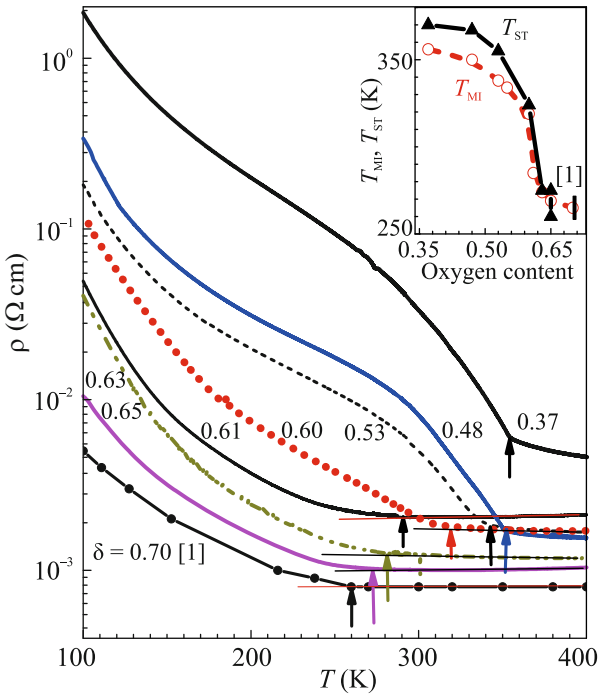

Fig. 2. (Color online) Temperature dependence of the resistivity of $NdBaCo_2O_{5+\delta}$ ($0.37 \le \delta \le 0.65$). Inset: the metal–insulator transition temperature T_{MI} and the spin-state transition temperature T_{ST} versus the oxygen content δ.

$RBaCo_2O_{5.50}$ compounds with the largest sizes of R^{3+} = La, Pr, and Nd ions exhibit the FM behavior at all temperatures below T_C, even in the AFM phase [24–26], while compounds with smaller sizes of R^{3+} ions demonstrate the AFM behavior [1–7]. These results confirm the effect of the ionic size of R on the FM state in layered cobaltites.

In Fig. 2, we show the temperature dependence of the resistivity $\rho(T)$ of $NdBaCo_2O_{5+\delta}$ at $0.37 \ge \delta \ge 0.65$ in the temperature range 100–400 K. For comparison, we present the $\rho(T)$ data for $\delta = 0.70$ [1]. The temperature dependence of the resistivity $\rho(T)$ exhibits a semiconducting behavior: $\rho(T)$ decreases monotonically with increasing temperature and oxygen content. After a sharp decrease in $\rho(T)$ above T_{MI} indicated in Fig. 2 by arrows, the sample passes to a state with the resistivity only slightly dependent on the temperature. In fact, the transition from the quasimetallic to the semiconductor state rather than the metal–insulator transition occurs [1, 2]. The derivative $d\rho/dT$ remains negative above T_{MI}, suggesting the semiconducting behavior of $\rho(T)$, possibly related to the polycrystalline structure of the sample.

In a narrow temperature range (~100–150K below T_{MI}), the resistivity of $NdBaCo_2O_{5+\delta}$ with $0.48 \ge \delta \ge 0.65$ can be described by the activation-type relationship [20]

$$\rho(T) = \rho_0 \exp(\Delta E/kT). \quad (1)$$

With an increase in δ, the activation energy ΔE characterizing the resistivity changes from $\Delta E \sim (50 \pm 10)$ meV to $\Delta E \approx 30$ meV for $\delta = 0.65$ (0.70). The pre-exponential factor also decreases from $\rho_0 \approx 3 \times 10^{-3}$ Ω cm, which is characteristic of a disordered medium, to the value $\rho_0 \approx 2 \times 10^{-4}$ Ω cm, which is larger than that typical of semiconductors. The positive magnetoresistance $MR = [\rho(H) - \rho(H = 0)]/\rho(H = 0)$ up to 2.5% at $H = 10$ kOe characteristic of semiconductors is observed in $NdBaCo_2O_{5.65}$ in the temperature range $T_C < T < T_{MI} \sim 250$ K.

It is interesting to note that $T_{MI}(\delta)$, $T_N(\delta)$, and $T_C(\delta)$ (see insets of Figs. 1 and 2), differing in magnitude by about 100 K, at different oxygen contents, have approximately the same form: they change slightly at $\delta \le 0.53$ and decrease steeply at $\delta > 0.60$. The changes in $\rho(T)$ decrease with an increase in δ. From 100 K to T_{MI}, the resistivity changes by almost three orders of magnitude at $\delta = 0.37$, whereas at $\delta = 0.65$, it changes by less than one order of magnitude. At $\delta = 0.65$, a heavily doped semiconductor–bad metal transition occurs with almost no change in the spin state. Qualitatively, the behavior of $\rho(\delta, T)$ agrees with changes in the effective magnetic moment $\mu_{eff}(\delta, T)$ (see below).

Magnetic methods are among the main ones for determining the spin states of Co^{3+} ions in cobaltites. The spin state of Co^{3+} ions is determined from the measurements of the paramagnetic susceptibility described by the Curie–Weiss law $\chi(T) \sim \mu^2_{eff}/(T - \theta_{PM})$ above and below T_{MI} [1–7]. For these purposes, the magnetic methods turn out to be rather complicated because it is difficult to distinguish the contribution of Co^{3+} ions in $RBaCo_2O_{5+\delta}$ and the PM contribution from rare earth ions R^{3+}. The discrepancies between the spin states of Co^{3+} ions reported in different publications are probably due to the fact that the latter contribution is ignored or is taken into account incorrectly (see [9]). It is usually assumed that this contribution coincides with that of free R^{3+} ions and is determined using the expression for the paramagnetic susceptibility $\chi = \mu^2_{eff}/3k(T - \theta_{PM})$, where μ_{eff} is the effective magnetic moment of the R^{3+} ion, k is the Boltzmann constant, and $\theta_{PM} = 0$ is the Weiss paramagnetic temperature [3, 6, 7, 27]. The values of μ_{eff} and θ_{PM} are determined on the basis of the saturation of magnetization at a high magnetic field at low temperatures [9, 28], which for rare earth ions R^{3+} is described by the Brillouin function [29]

$$M = N_A g \mu_B J B_S(x), \quad (2)$$

where $B_S(x)$ is the Brillouin function, N_A is the Avogadro number, $x = g\mu_B JH/(k(T - \theta_{PM}))$, g is the Landé g-factor, μ_B is the Bohr magneton, J is the total mag-

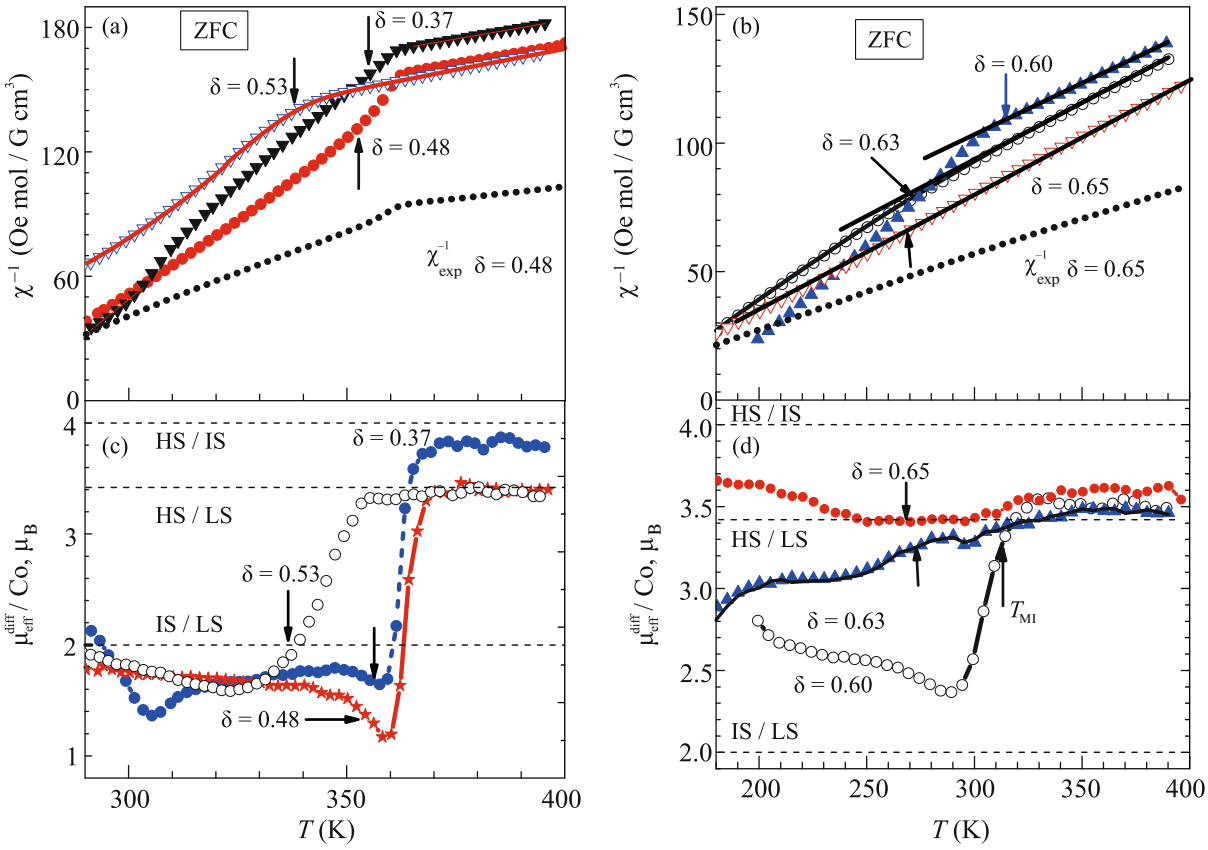

Fig. 3. (Color online) Temperature dependence of the inverse paramagnetic susceptibility $\chi^{-1}(T)$ and of the differential magnetic moment μ^{dif}_{eff}/Co of $NdBaCo_2O_{5+\delta}$ ($0.37 \le \delta \le 0.65$). Symbols denote the data at $H = 10$ kOe and lines correspond to $H = 1$ kOe or 50 kOe (see the main text). The paramagnetic contribution from Nd^{3+} ions is subtracted. The arrows indicate the metal–insulator transition temperatures.

netic moment of an R^{3+} ion, and H is the applied magnetic field. In this work, we assume that the PM contribution from Nd^{3+} ions in $NdBaCo_2O_{5+\delta}$ is independent of δ and is described by Eq. (2) at $\theta_{PM} = -18$ K, as in $NdBaCo_2O_{5.48}$ [14].

In Figs. 3a and 3b, the symbols denote the temperature dependence of the inverse paramagnetic susceptibility $\chi^{-1}(T)$ of $NdBaCo_2O_{5+\delta}$ ($\delta = 0.37$–0.65, $H = 10$ kOe), determined by the subtraction of the PM contribution from the Nd^{3+} ion. Circles are the measured values of $\chi^{-1}_{exp}(T)$ at $\delta = 0.48$ and 0.63. All samples were cooled at $H = 0$ from 300 to 10 K, and the magnetization was measured up to 400 K at $H = 1$, 10, and 50 kOe. The solid lines show the $\chi^{-1}(T)$ data for $\delta = 0.53$ at $H = 50$ kOe and for $\delta = 0.65$ at $H = 1$ kOe, which hardly differ from the $\chi^{-1}(T)$ values at $H = 10$ kOe. The same data were obtained for other values of δ. These results prove the applicability of Eq. (2) for determining the PM contribution from Nd^{3+} ions.

The temperature dependences $\chi^{-1}(T)$ for $\delta = 0.37$–0.60 are nearly the same and are similar to the observed dependences $\chi^{-1}(T)$ in known layered cobaltites with $\delta \approx 0.5$. In these samples, it is almost impossible to separate a linear segment in the $\chi^{-1}(T)$ plots. In fact, this means that the behavior of $\chi^{-1}(T)$ cannot be described at a constant value of $\mu_{eff}(T)$, and the transition is accompanied by the changes in $\mu_{eff}(T)$ with temperature. On the other hand, for $\delta = 0.63$ and 0.65 above and below T_{MI}, a linear behavior of $\chi^{-1}(T)$ is observed. To reveal the features of the metal–insulator transition, the differential values μ^{dif}_{eff}/Co(T) were determined. The values of $\chi^{-1}(T)$ were measured with an interval of $\Delta T = 5$ K, and at each step, the differential values $\mu^{dif}_{eff}/Co^{3+}(T)$ were determined taking into account the contribution of the specific content of Co^{2+} and/or Co^{+4} ions for all values of δ (Figs. 3c and 3d).

In a certain temperature range below 400 K, μ^{dif}_{eff}/Co at $\delta = 0.37$–0.60 remains constant (Figs. 3c and 3d). The temperature at which the slope of the $\chi^{-1}(T)$ plot changes sharply (which corresponds to a

sharp decrease in μ_{eff}^{dif}/Co) is accepted as the metal–insulator transition temperature T_{ST} related to the spin-state transition. This temperature, T_{ST}, is approximately 10–15 K higher than the T_{MI} temperature at $\delta = 0.37$–0.53 (see inset of Fig. 2). These discrepancies are explained by the contribution of intergranular resistance to the resistivity of polycrystals. At $\delta = 0.60$–0.65, neither $\rho(T)$ shown in Fig. 2 nor $\chi^{-1}(T)$ plotted in Figs. 3a and 3b demonstrates any pronounced transition boundary. According to the intuitive definition of this boundary, T_{ST} and T_{MI} coincide with each other. Below 400 K, we observe a decrease in $\chi^{-1}(T)$ proportional to the temperature at $\delta = 0.63(0.65)$ above and below T_{MI}. The slopes of the $\chi^{-1}(T)$ curve above and below T_{MI} are slightly different (see the solid lines plotted through the symbols corresponding to $\delta = 0.63$ and 0.65 in Fig. 3b). Their behavior indicates that a small change in the spin state of Co^{3+} ions occurs near T_{MI}.

In the metallic phase ($\delta = 0.37$–0.65) at $T > T_{MI}$ (Figs. 3c and 3d), $\mu_{eff}^{dif}/Co^{3+} = (3.43 \pm 0.02)\mu_B$ is independent of the oxygen content and corresponds to the HS/LS state of Co^{3+} ions in the ratio of 1 : 1. The significant deviation of μ_{eff}^{dif}/Co from this state at $\delta = 0.37$ and its slight deviation at $\delta = 0.60$–0.65 are explained by the different contributions from Co^{2+} and Co^{4+} ions. Co^{2+} ions are always in the HS ($S = 3/2$) state because of a weaker crystal field than that for Co^{3+} ions, whereas Co^{4+} ions are always in the LS ($S = 1/2$) state because of a stronger crystal field [30]. With an increase in the content of Co^{2+} or Co^{4+} ions, the deviation of μ_{eff}^{dif}/Co^{3+} from the HS/LS state increases, which is in reasonable agreement with the calculations of the contribution from Co^{2+} and Co^{4+} ions.

In the semiconductor phase at $T_C < T < T_{MI}$ and $\delta = 0.37$–0.53 (Fig. 3c), the compounds are in the IS/LS state, and most of the Co^{3+} ions are in the LS state. Then, an abrupt transition to the HS/LS state occurs in a narrow temperature range. At $\delta = 0.60$–0.63 (Fig. 3d), the μ_{eff}^{dif}/Co^{3+} values exceed those corresponding to the IS/LS state of Co^{3+} ions in a ratio of 1 : 1; i.e., most of the Co^{3+} ions are in the IS state.

Next, in Figs. 3a and 3b, we identify the fragments with a nearly linear temperature dependence on $\chi^{-1}(T)$ curves, find the values of μ_{eff}^{dif}/Co^{3+} from the Curie–Weiss law (lines *1* and *2* in Fig. 4), and determine the Weiss paramagnetic temperature θ_{PM} (lines *3* and *4* in Fig. 4) above and below T_{MI} depending on the oxygen content δ (Fig. 4). In the metallic phase (line *1* in Fig. 4) at $T > T_{MI}$, $\mu_{eff}/Co^{3+} = (3.43 \pm 0.02)\mu_B$ does not depend on the oxygen content $\delta = 0.37$–0.65 and corresponds to the HS/LS state of Co^{3+} ions in the ratio of 1 : 1. The significant deviation of μ_{eff}/Co from

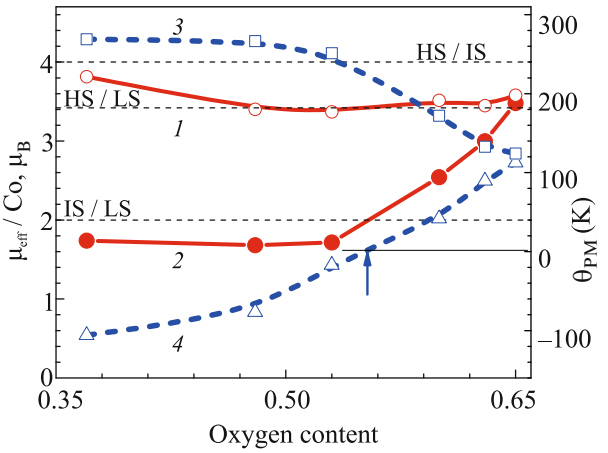

Fig. 4. (Color online) (Lines *1* and *2*) Effective magnetic moment μ_{eff}/Co and (lines *3* and *4*) the paramagnetic temperature θ_{PM} of $NdBaCo_2O_{5+\delta}$ cobaltite in the (lines *1* and *4*) metallic and (lines *2* and *3*) semiconducting phases versus the oxygen content δ.

this state at $\delta = 0.37$ and its slight deviation at $\delta = 0.65$ are explained above by different contributions from Co^{2+} and Co^{4+} ions. In the paramagnetic phase at $T_C < T < T_{MI}$, μ_{eff}/Co (line *2* in Fig. 4) at $\delta = 0.37$–0.53 is constant; as δ increases further to 0.65, μ_{eff}/Co increases to the μ_{eff}/Co value at $T > T_{MI}$. With an increase in the Co^{4+}/Co^{3+} ratio to 15/85 ($\delta = 0.65$), the semiconductor–bad metal transition (Fig. 2) occurs without a change in the spin state. The results on μ_{eff}/Co agree with the μ_{eff}^{dif}/Co data shown in Fig. 3.

Since the Weiss paramagnetic temperature θ_{PM} is related to the characteristics of the exchange interaction [29], determining θ_{PM} below and above T_{MI}, one can obtain information about the exchange interaction depending on the oxygen content. In the semiconducting phase at $T_C < T < T_{MI}$, as δ increases, the values of θ_{PM} decrease from about 260 to 100 K at $\delta = 0.65$ (line *3* in Fig. 4). In the metallic phase, θ_{PM} increases from $\theta_{PM} \approx -100$ K to positive values (line *4* in Fig. 4). At $\delta = 0.65$, θ_{PM} is about 110 K, coinciding with θ_{PM} at $T < T_{MI}$. The change in the sign of θ_{PM} at $\delta \approx 0.55$–0.6 means that the exchange interaction changes from AFM + FM to FM exchange and the FM exchange becomes stronger with an increase in δ.

As the oxygen content increases, both the magnetization $M_{max}(\delta)$ at T_N (Fig. 1) and the spontaneous magnetization M_s (according to our preliminary data) first decrease to a minimum at $\delta = 0.60$ and then increase. The spontaneous magnetization of $NdBaCo_2O_{5+\delta}$ first decreases from $M_s \approx 0.40\mu_B$ at $\delta = 0.48$ to a minimum of $M_s \approx 0.2\mu_B$ at $\delta = 0.60$ and then increases to $0.85\mu_B$ at $\delta = 0.65$. The nonmonotonic behavior of $M_{max}(\delta)$ and $M_s(\delta)$ suggests the existence of competing FM and AFM interactions in these

compounds. The FM exchange can be caused by the Co^{3+}–O–Co^{4+} double exchange mechanism [30] or, according to the empirical Goodenough–Kanamori rule, by the presence of Co^{3+}–O–Co^{4+} FM superexchange interactions [31] as well as of the Co^{3+}–O–Co^{3+} AFM superexchange [32].

The temperature and field dependences of the magnetization of $PrBaCo_2O_{5+\delta}$, where $0.35 \le \delta \le 0.8$ [15], and of $NdBaCo_2O_{5+\delta}$, where $0.37 \le \delta \le 0.65$ (Fig. 1), are similar; T_C and T_N, depending on δ, also decrease by about 100 K, and most sharply at $\delta > 0.6$ [15]. The magnetic behavior of $GdBaCo_2O_{5+\delta}$ also changes noticeably when the oxygen content is $\delta > 0.55$. The authors of [3] suggest that such a change is a manifestation of a change in the positions of spins of Co^{3+} and Co^{4+} ions. One can suppose that the features appearing at $\delta \sim 0.6$ are also inherent in other layered cobaltites; they are due to a change in the exchange interaction from AFM + FM to FM behavior with an increase in the oxygen content.

The values of $T_C(\delta)$ and $T_N(\delta)$ for $NdBaCo_2O_{5+\delta}$ differ by about 20 K and have similar δ dependences (see inset of Fig. 1). The result seems to be natural, since the FM state smoothly transforms to the AFM state within a narrow temperature range. A slight change in $T_C(\delta)$ and $T_N(\delta)$ for $NdBaCo_2O_{5+\delta}$ at δ up to 0.53 and its strong decrease above $\delta = 0.6$, as well as the nonmonotonic behavior of the magnetization $M_{max}(\delta)$ (Fig. 1), can be qualitatively explained, in our opinion, by a change in the nature of the exchange interactions. At $\delta < 0.53$, AFM + FM interactions are present; therefore, M_{max} and T_N decrease, but slightly. The dominant role of FM interactions at $\delta > 0.6$ leads to an increase in the magnetization $M_{max}(\delta)$, to a decrease in $T_C(\delta)$ and $T_N(\delta)$ by about 100–150 K with an increase in the Co^{3+}–O–Co^{4+} FM exchange, and, accordingly, to a weakening of the Co^{3+}–O–Co^{3+} AFM exchange with an increase in the contribution of the magnetization related to the Co^{4+} ions.

However, an alternative explanation for the behavior of $T_C(\delta)$ is also known [33]. It is usually assumed that a transition to the AFM state occurs at $T = T_N$, although the behavior of the magnetization $M(T)$ is not characteristic of an antiferromagnet: the magnetization remains nonzero well below T_N. The behaviors of the magnetization $M(T, H = 1\ kOe)$ of $NdBaCo_2O_{5.48}$ near T_C (Fig. 1) and the spontaneous magnetization M_s are also not characteristic of a pure ferromagnet. The spontaneous magnetization of $NdBaCo_2O_{5+\delta}$ at $\delta \approx 0.5$ arises at $T \sim 300$ K, which is 15–20 K higher than T_C determined from dM/dT (see inset of Fig. 3 [14]). According to our preliminary data, a similar behavior of T_C and M_s is characteristic of compounds with other values of δ (Fig. 1). Numerical calculations allowed Wu [33] to assume that a noncollinear AFM state arises at T_N, and no transition to the FM state occurs at $T = T_C$, whereas a smooth transition from the PM state to the canted, noncollinear AFM state occurs, and a transition to another collinear AFM state occurs below T_N. According to the muon spectroscopy data, another AFM structure arises in $NdBaCo_2O_{5.50}$ at approximately 100 K below $T_N = 265(5)$ K [13].

CONCLUSIONS

Polycrystals of layered $NdBaCo_2O_{5+\delta}$ cobaltites with different oxygen content $0.37 \le \delta \le 0.65$ have been synthesized by the solid-state reaction technique. The metal–insulator transition in $NdBaCo_2O_{5+\delta}$ occurs when the spin state of Co^{3+} ions changes from HS/LS in the metallic phase to the IS/LS state in the semiconducting phase, as well as in the related $RBaCo_2O_{5.5}$ compound, where R = Gd and Tb [9, 28]. With an increase in δ, the spin states of Co^{3+} ions in the semiconducting phase of $NdBaCo_2O_{5+\delta}$ approach those characteristic of the HS/LS state. The observed deviations of the spin states from the HS/LS state are in reasonable agreement with the possible effects introduced by Co^{2+} and/or Co^{4+} ions.

The ferromagnetic behavior of $NdBaCo_2O_{5+\delta}$ below T_N in the antiferromagnetic phase is explained by the large size of Nd^{3+} ions.

We argue that the decrease in T_N, T_C, T_{MI}, and T_{ST} by about 100–150 K, the nonmonotonic behavior of the magnetization $M_{max}(T = T_N)$, and its increase at $\delta > 0.53$–0.6 are caused by a change in the exchange interactions between Co^{3+} and Co^{4+} ions from AFM + FM to FM exchange with an increase in δ.

ACKNOWLEDGMENTS

We are grateful to A.V. Telegin for fruitful discussions and to A.V. Korolev for his assistance with the magnetic measurements.

FUNDING

This work was supported by the Ministry of Science and Higher Education of the Russian Federation (state assignment no. AAAA-A18-118020290104-2, project Spin) and partially by the Russian Foundation for Basic Research (project no. 20-02-00461).

CONFLICT OF INTEREST

The authors declare that they have no conflicts of interest.

REFERENCES

1. A. Maignan, C. Martin, D. Pelloquin, N. Nguyen, and B. Raveau, J. Solid State Chem. **142**, 247 (1999).

2. C. Martin, A. Maignan, D. Pelloquin, N. Nguyen, and B. Raveau, Appl. Phys. Lett. **71**, 1421 (1997).
3. A. A. Taskin, A. N. Lavrov, and Y. Ando, Phys. Rev. B **71**, 134414 (2005).
4. C. Frontera, J. L. García-Muñoz, C. Ritter, D. Martín y Marero, and A. Caneiro, Phys. Rev. B **65**, 180405(R) (2002).
5. Y. Moritomo, T. Akimoto, M. Takeo, A. Machida, E. Nishibori, M. Takata, M. Sakata, K. Ohoyama, and A. Nakamura, Phys. Rev. B **61**, 13325(R) (2000).
6. Z. X. Zhou and P. Schlottmann, Phys. Rev. B **71**, 174401 (2005).
7. M. Baran, V. I. Gatalskaya, R. Szymczak, S. V. Shiryaev, S. N. Barilo, K. Piotrowski, G. L. Bychkov, and H. Szymczak, J. Phys.: Condens. Matter **15**, 8853 (2003).
8. N. B. Ivanova, S. G. Ovchinnikov, M. M. Korshunov, I. M. Eremin, and N. V. Kazak, Phys. Usp. **52**, 789 (2009).
9. N. I. Solin, S. V. Naumov, and V. A. Kazantsev, J. Exp. Theor. Phys. **130**, 690 (2020).
10. C. Frontera, J. L. García-Muñoz, A. E. Carillo, M. A. G. Aranda, I. Margiolaki, and A. Caneiro, Phys. Rev. B **74**, 054406 (2006).
11. R. D. Shannon, Acta Crystallogr., A **32**, 751 (1976).
12. F. Fauth, E. Suard, V. Caignaert, and I. Mirebeau, Phys. Rev. B **66**, 184421 (2002).
13. A. Jarry, H. Luetkens, Y. G. Pashkevich, P. Lemmens, H.-H. Klaus, M. Stingaciu, E. Pomjakushina, and K. Conder, Phys. B (Amsterdam, Neth.) **404**, 765 (2009).
14. N. I. Solin and S. V. Naumov, JETP Lett. **114**, 150 (2021).
15. S. Ganorkar, K. R. Priolkar, P. R. Sarode, and A. Banerjee, J. Appl. Phys. **110**, 053923 (2011).
16. L. Landau, Phys. Zs. Sowjet. **4**, 675 (1933).
17. D. D. Khalyavin, O. Prokhnenko, N. Stüßer, V. Sikolenko, V. Efimov, A. N. Salak, A. A. Yaremchenko, and V. V. Kharton, Phys. Rev. B **77**, 174417 (2008).
18. D. Chernyshov, V. Dmitriev, E. Pomjakushina, K. Conder, M. Stingaciu, V. Pomjakushin, and A. Podlesnyak, Phys. Rev. B **78**, 024105 (2008).
19. P. Miao, X. Lin, S. Lee, Y. Ishikawa, S. Torii, M. Yonemura, T. Ueno, N. Inami, K. Ono, Y. Wang, and T. Kamiyama, Phys. Rev. B **95**, 125123 (2017).
20. L. S. Lobanovskii, I. O. Troyanchuk, H. Szymczak, and O. Prokhnenko, J. Exp. Theor. Phys. **103**, 740 (2006).
21. S. Vlakhov, N. Kozlova, L. S. Lobanovskii, R. Wawryk, and K. A. Nenkov, Phys. Rev. B **84**, 184440 (2011).
22. C. Frontera, J. L. García-Muñoz, A. E. Carrillo, C. Ritter, D. M. y Marero, and A. Caneiro, Phys. Rev. B **70**, 184428 (2004).
23. J. C. Burley, J. F. Mitchell, S. Short, D. Miller, and Y. Tang, J. Solid State Chem. **170**, 339 (2003).
24. E.-L. Rautama, V. Caignaert, Ph. Boullay, A. K. Kundu, V. Pralong, M. Karppinen, C. Ritter, and B. Raveau, Chem. Mater. **21**, 102 (2009).
25. Md. M. Seikh, V. Pralong, O. I. Lebedev, V. Caignaert, and B. Raveau, J. Appl. Phys. **114**, 013902 (2013).
26. E.-L. Rautama, V. Caignaert, P. Boullay, A. K. Kundu, V. Pralong, M. Karppinen, and B. Raveau, Chem. Mater. **21**, 102 (2009).
27. S. Kolesnik, B. Dabrowski, O. Chmaissem, S. Avci, J. P. Hodges, M. Avdeev, and K. Swierczek, Phys. Rev. B **86**, 064434 (2012).
28. N. I. Solin, S. V. Naumov, and S. V. Telegin, JETP Lett. **107**, 203 (2018).
29. S. V. Vonsovskii, *Magnetism* (Nauka, Moscow, 1971; Wiley, New York, 1971), Chap. 9.
30. C. Zener, Phys. Rev. **81**, 440 (1951).
31. J. Goodenough, *Magnetism and the Chemical Bond* (Wiley Intersci., New York, 1963).
32. P. W. Anderson, Phys. Rev. **115**, 2 (1959).
33. H. Wu, J. Phys.: Condens. Matter **15**, 503 (2003).

Translated by K. Kugel